CONF-9210287--1

BNL--48177

DE93 005592

High-Energy Pion Beams: Problems and Prospects

R.E. Chrien

Dept. of Physics, Brookhaven National Laboratory, Upton N. Y. 11973

The investigation of relatively unexplored research areas with high energy pion beams requires new facilities. Presently existing meson factories such as LAMPF, TRIUMF and PSI provide insufficient pion fluxes above the 3,3 resonance region for access to topics such as strangeness production with the (π, K) reaction, baryon resonances, rare meson decays, and nuclear studies with penetrating pion beams. The problems and prospects of useful beams for these studies will be reviewed, both for existing facilities such as the AGS and KEK, and for possible future facilities like KAON and PILAC.

I. INTRODUCTION

The research areas which can be addressed with pion beams in the 1.0 GeV/c range, or above, have been identified not only in this workshop, but in many others held in connection with proposed new facilities. The reviews of the physics research for an advanced hadron facility[1], for KAON[2], and for the PILAC Users Group Report[3], have examined these possibilities in some detail.

This paper will focus on a few of the practical problems of usage of such beams, drawing mostly on the experience obtained at the AGS over the past fifteen years. The availability of such facilities as the AGS and KEK has permitted a limited progress in the attack on interesting areas and have indicated which ones might be most fruitful to explore. In this paper, those topics include 1) strangeness production with the (π^+, K^+) reaction; 2) nuclear physics with pions; 3) the fundamental nature of the hadronic force (QCD), and 4) the role of other mesons, such as the η, in nuclear physics. In each of these areas, there are ongoing programs at existing facilities. The long-range future exploitation of these areas is problematical; for the next three to five years, however, sufficient resources remain for a number of significant experiments.

This review does *not* cover the diverse programs of the presently-existing meson "factories" which operate in the region of dominance of the Δ-isobar in pion-nucleus interactions. However, experiments involving hadronic probes other than pions will be included as secondary production of protons, antiprotons, and kaons supplements the copious pion intensities available from proton synchrotrons in the multi-GeV region.

II. SOME PROPERTIES OF SECONDARY PARTICLE BEAMS

In this section, reference is made to some aspects of secondary-particle production which are useful to keep in mind for research applications. These aspects are described fairly well in the well-known empirical formulation of J.R. Sanford and C.L. Wang[4]. Although there are known deficiencies in this formulation[5],[6], it describes secondary production well enough to be useful in a comparison of facilities (It should be noted that while the Sanford-Wang formula applies to beryllium targets, the typical AGS target is platinum). Figure 1 shows one feature to keep in mind; for 1 GeV pions produced by primary proton interactions of KEK or AGS energies— i.e., 12 to 24 GeV, the negative particle production is nearly as large as the positive particle production. There is less than a factor of 2 between π^+ and π^- production at $\theta = 5°$, for 23

GeV incident proton kinetic energy. It has also been observed at the AGS that the convenient Sanford-Wang parameterization gives a reasonable production for the intensity scale, as well as the shape, for the secondary particle production.

It is interesting to contrast the negative pion production with that of PILAC, for example, where the π^- production is down by a factor of 20 compared to π^+ [3], due to the much lower primary proton energy.

A second point to bear in mind is the relative productions of pions, kaons and antiprotons. As shown in Fig. 2, calculated under the same conditions as Fig. 1, these secondary particles all peak at relatively low momenta, with peak intensities of $\sim 2 : 0.07; 0.008$ particles/GeV/c/sr/interacting primary proton, for π's, K's, and $\bar{p}$'s, respectively. The length of beam line, of course, will profoundly affect the intensities for π and K mesons.

A final point involves the secondary pion production as a function of primary proton energy. Fig. 3 shows a comparison of the AGS at 23 GeV proton kinetic energy to KEK (12 GeV) for π^+ production as 5°. A roughly linear dependence on primary proton energy is inferred from the graph, for the π^+ production at 1.0 GeV/c, with the AGS flux exceeding that for KEK by a factor of two. This linear dependence has been confirmed by Amann *et al*[6].

This section concludes by examination of a table of the presently operating beam lines providing pions (or kaons, protons, and antiprotons) used in nuclear physics research. Fig. 4, shows 14 lines which are in operation at the KEK[7] and the AGS[8], and lists their intensities for the indicated particles. Half of those lines are separated beams, using electrostatic separators to provide mass selection on the secondary particles. Many applications require precise particle identification and this feature is enhanced by the use of separators. The KEK lines K2, K5, and K6, and the AGS LESB-II and D6 lines are heavily used in nuclear physics experiments. These lines feature excellent particle separation between pions, kaons, and protons. Two of these lines at the AGS are quite new: the D6 2 GeV/c line was specifically designed for H-particle searches and $\Lambda\Lambda$ experiments requiring a clean K^-K^+ trigger[9]. It features high kaon intensities (better than $10^6 K^-$/spill) and good separation (1 : 1 for K^-/π^-). The LESB-III line has replaced the venerable LESB-I line, which was used for many hypernuclear experiments at the AGS in the period 1976 to 1989. THE LESB-III provides a K^+/π^+ ratio of 2 : 1 and is being used for the rare decay process, $K^+ \rightarrow \pi^+\nu\bar{\nu}$.

One notes from this table that typical momentum spreads for these lines are 5%, and the intensities scale between KEK and the AGS as predicted by Sanford-Wang. The LESB-III, LESB-II, and D6 lines provide the highest pion fluxes currently available. LESB-III and D6 are also outfitted with target stations capable of taking 10^{13} primary protons per spill and have suitably radiation-hardened front-end magnets.

III. HYPERNUCLEAR STUDIES WITH PION BEAMS

The pioneering experiments in the utilization of the (π^+, K^+) reaction for hypernuclear production were done at the AGS and form good examples of the use of high energy pion beams.

The (π^+, K^+) reaction has been demonstrated to be an excellent way of producing hypernuclei across a wide range of target mass numbers. The reaction takes advantage of a peak in the elementary production cross section at a pion momentum near 1.05 GeV/c to create hypernuclei by associated production. The high momentum transfer (about 300 MeV/c at 10° for a typical target) favors the formation of high-spin states. The affect of nuclear absorption favors the transformation of a nucleon to a Λ from valence neutron states. Thus the dominant spectral appearance is what one expects to get from coupling a Λ in the various shells (s, p, d, f; g ...) to valence neutron hole states. Although the higher shells predominate, there is sufficient cross section to populate even the s_Λ ground state configuration for quite heavy nuclides. The classic example [10] is shown in Fig. 5 for ^{89}Y; here the various Λ single particle states, as shown, couple to the predominant $g_{9/2}$ neutron hole state as shown.

These elementary single-particle states are highly fragmented and the resolution is inadequate to display the fine structure. Each particle-hole configuration is broken up into multiplets of states split by Λ spin-dependent interactions. The pioneering (π, K) spectra were first obtained with a modest intensity and limited running time, but their most serious deficiency is lack of adequate resolution. The spin dependent Λ-nuclear interactions are small and thus the spin splittings are small. Another complication is that the hole strength is never concentrated into one configuration, but is spread over a number of configurations. An example is the $^{12}_{\Lambda}C$ spectrum of Fig. 6, where the s-shell Λ particle is coupled to $p_{3/2}$ carbon hole state. The hole strength is spread over the $3/2^-$ gs, the $1/2^-$ 2.00 MeV, and the $3/2^-$ 4.80 MeV states of ^{11}C as shown. The relative population of these weaker excited states is only hinted at in the figure; the actual departure of the observed strength of these excited states from the 40% predicted by the weak coupling limit, and their positions, would be a measure of the mixing induced by the ΛN interaction.

Another illustration of the necessity for higher resolution and higher intensity is shown in Fig. 7 for ^{51}V; this spectrum was the result of a 23 hour run. The data are shown with the indicated dominant $f_{7/2}$ and $d_{3/2}$ hole strengths, which are separated by 2.6 MeV. The observed spacing indicates a Λ shell separation of about 7.0 MeV in this mass region.

A summary of the ground state production cross sections [10] is given in Fig. 8, which illustrates the energy precisions ($\sim$ 1 MeV) and cross section sensitivities $\sim$ (0.5 μb/sr) of this experiment. Fig. 9 shows the π^+ intensities and run times available for this experiment, and it indicates the use of relatively thick targets. Beam contamination with muons and electrons is a serious problem with pion beams, and especially so when precise cross sections are desired. At the higher intensities shown in the table an absorber was placed near the mass slit of the beam separator to minimize electron contamination.

The (π^+, K^+) program is being pursued at KEK beam lines K2 and K6 with pion intensities comparable to the BNL experiments. One interesting aspect of the KEK program is the use of the (π^+, K^+) reaction to produce polarized Λ particles and polarized hypernuclei. The initial attempt of Ejiri and his collaborators in attacking this problem was to measure the polarization of the emitted Λ in the (π^+, K^+) reaction on ^{12}C[11]. Their detector, called ROYAL, is shown in Fig. 10, and consists of a layer of dE/dx and E scintillators which detect the π^- and p from the Λ charged particle decay mode. The decay asymmetry with respect to the (π, K) reaction plane is a measure of the polarization P, and the result is shown in Fig. 11. Here the polarization in the region of quasifree Λ production approaches the value attained in free space; in the bound state region, the pionic decay of hypernuclear states gives a small asymmetry, while at high excitations, depolarization from ΛN scattering processes can be expected. The next step[12] in such studies was an examination of the non-mesonic decay asymmetry from the bound states of a polarized ^{12}C hypernucleus.

The PILAC Users Group Report [3] describes a facility which is optimized for (π, K) studies—a pion linear accelerator coupled to LAMPF. The future of PILAC is uncertain in the present funding atmosphere. Phil Pile[13] has outlined an alternative to PILAC and stressed the capabilities of the AGS to accommodate a π, K program. If we assume the PILAC beam channel parameters $\ell = 30$ m, $\Delta p/p = 1\%$, $\Delta\Omega = 3$ msr, a 6 cm Pt production target, $\theta = 5^\circ$ production angle, and a 10^{13} protons/spill then $2.2 \times 10^8 \pi^+$/spill or about $0.7 \times 10^8 \pi^+$/sec could be provided. If a state-of-theart, high resolution EPICS-style spectrometer were added, a net gain of 33 over the old experiment event rate could result. Clearly much of the PILAC-envisioned (π, K) program could be accomplished with such a facility.

IV. HIGH ENERGY PION NUCLEON SCATTERING

In the past two decades, studies of hadronic reactions on nuclei have been the almost exclusive province of the so-called meson factories—the Paul Scherrer Institute (PSI), TRIUMF, and the Los Alamos Meson Physics Facility (LAMPF). These institutions provide intense pion beams in an energy regime dominated by the Δ isobar. Because of the (3,3) resonance, the physics range of pion- nucleon and pion-nuclear interactions has been defined and limited by its dominance.

Interactions above the resonance region are qualitatively different; due to the presence of other baryon resonances with different quantum numbers and decay channels there results a marked change in the nature of the two-body pion-nucleon interaction. The larger mean-free path of off-resonance pions allows access to the nuclear interior and different portions of the nuclear volume are thereby sampled. Fig. 12 , taken from ref.[14], gives some indication of these features.

The usefulness of penetration by hadronic probes has been illustrated by the K^+ meson; the K^+-nucleon interaction has been used to establish nuclear medium alterations of elementary interactions. The pioneering experiments of Marlow and collaborators [14],[15] at the AGS a decade ago illustrate some of the problems associated with the scattering of higher-energy pions and kaons. Fig. 13 shows a time-of-flight measurement of the BNL LESB-I (a predecessor of LESB-III) beam, obtained from that work. One can see the clean kaon peak, well separated from contaminants because of the large mass difference between kaons and lighter particles. The pions, electrons, and muons in the beam are however difficult to separate because of their nearly identical beta values at the 800 MeV/c of the Marlow experiments. The muons are difficult to separate from pions at almost any momentum because of the small energy release in pionic decay.

The pion cross sections from the Marlow experiment were obtained by renormalizing the data against (π, p) elastic scattering [14], as is evident from Fig. 14. The renormalizing factor implied in that figure suggests a contamination of 50% muons, which is perhaps not so surprising since in the Marlow experiment the beam was timed for kaons and the pion data obtained as a by-product.

The fact is that an unavoidable muon halo accompanies any pion beam, and the effective beam phase space is larger because of that halo, which is caused by small- angle pion decays. This is indicated in Fig. 15, which shows a pion beam (620 MeV/c) time-of-flight spectrum for two detectors with an area ratio of 100 : 1, but with an identical time-of-flight resolution, $\sigma \approx 280$ psec, as measured with kaons. The broadening is obviously dependent on detector size. In this example, the muon-pion time difference over the path length of 11.5 meters is 500 psec. Muon contamination is an obvious problem in pion beam monitoring; in the next section an experiment is described in which its importance becomes crucial.

V. ETA-PRODUCTION AND AN EXPERIMENT IN CHARGE-SYMMETRY BREAKING

The PILAC Users Group Report stresses the importance of tests of the Standard Model involving η-meson decays. Pion beams near 750 MeV/c strongly excite the $S_{11}(1535)N^*$ resonance, which decays by η emission with a branching ratio of about 50%. This fact and the parameters of the LESBII beam line (see Fig. 4) suggest the possibility of installing a tagged η-production facility at the AGS for studying rare eta decays. It has been estimated [16] that 10^9 tagged etas per day could be produced with a π^+ beam of 10^9/spill (3×10^8/sec) on a deuterium target. At that level a number of interesting tests of fundamental symmetries and violations of the Standard Model become interesting. These include tests of C, P, CP, T, and CPT. Further new physics may be found in the role of leptoquarks which could boost decays to lepton pairs such as $\eta \rightarrow e^+e^-$, and in decays of the type $\eta \rightarrow \mu e$, which test lepton family number violations.

The feasibility of an AGS eta-source is part of Experiment 890 "A New Test of Charge Symmetry in $\pi d \rightarrow NN\eta$", by Nefkens, Chrien, and Peng. This experiment is designed to measure charge symmetry breaking by comparing the η production rate of $\pi^- d \rightarrow nn\eta$ against $\pi^+ d \rightarrow pp\eta$. QCD relates charge symmetry in nuclear physics to the up-down quark mass difference; this mass difference also induces meson mixing; specifically ρ^0-ω mixing and π^0-η mixing. The comparison of the symmetry ratios

$$R_1 = \frac{d^2\sigma(\pi^- d \rightarrow nn\eta)}{d^2\sigma(\pi^+ d \rightarrow pp\eta)}$$

and

$$R_2 = \frac{d^2\sigma(\pi^- d \rightarrow nn\pi^0)}{d^2\sigma(\pi^+ d \rightarrow pp\pi^0)}$$

for the same recoil kinematics for the proton and neutron pair reveal asymmetries between the $NN\eta$ and $NN\pi^0$ interactions. Quark model calculations give $R_1 < 1$ and $R_2 > 1$.

This experiment uses the η-spectrometer successfully employed by J.C. Peng [17]; a diagrammatic representation of this device is shown in Fig. 16. It consists of a pair of BGO converters, wire chambers to locate the shower vertices determining the opening angle of the photon pair, and sodium iodide detectors to measure the total energy of the shower. A requirement is careful beam monitoring to ensure equality between the pion beams of positive and negative polarity. The experiment layout of Fig. 17 shows monitors which are used to measure the pion scattering from protons and deuterons, a time-of-flight monitor for the beam particles, and a range spectrometer to isolate the Bragg ionization peak for the muon content of the beam.

In this experiment it is important to measure beam asymmetries between positive and negative pion production, so that instrumental asymmetries are not confused with valid charge symmetry-breaking effects. Experience has shown that tuning the beam may introduce asymmetries, and careful attention must be paid to beam contaminants. Fig. 18 shows how electron contamination, for example, is quite sensitive to separator tune. The figure shows time-of-flight profiles for a) a separator magnetic field set to 5% *below* optimum pion tune and b) 10% above the optimum. These tests, carried on at LESB-II in the summer of 1992, reinforce the necessity to measure and correct for the beam contaminants, which may change with beam polarity.

VI. QCD-RELATED NUCLEAR MEDIUM EFFECTS

While the emphasis here has been on pion beams in the region near 1.0 GeV/c, there are experiments at much higher energies which may be sensitive to QCD effects manifested at large momentum transfers. Currently in progress at the AGS, for example, is Experiment 852, which is a BNL-Penn State-Tel Aviv collaboration [18]. This experiment is designed to measure the $p+p \rightarrow p+p$ and $\pi^+ + n \rightarrow p + \pi^+ + \pi^-$ quasi free processes and compares nuclear medium cross sections against those for free space. Fig. 19 shows the results of an earlier experiment of Carroll *et al* [19] which displays the ratio of medium to free-space cross sections, termed nuclear transparency, as a function of beam momentum. For large transverse momentum transfer, the protons which participate in such processes are characterized by color-charge and color-field distributions confined to small spatial dimensions, and the cross section for soft initial and final state interactions decreases as the energy scale increases. At high energies, QCD predicts that the transparency $\mathcal{T}$ increases toward unity. The initial results show a maximum in $\mathcal{T}$ at an intermediate momentum, and a subsequent decline as the momentum is increased. This unexpected behavior has stimulated further measurements, which are now in progress at the AGS C-1 beam line.

VII. FUTURE PLANS

At the time of this review, there are no definite plans for the provision of new facilities for nuclear physics research in hadronic interactions. For some time the construction plans for the "KAON" facility[2] in Vancouver have been in abeyance. "KAON" would provide a set of beam lines[20], shown in Fig. 20, which offer separated beams of pions, kaons, and antiprotons ranging from 0.55 GeV/c up to 21 GeV/c, and with pion intensities up to 10^{11} sec^{-1}. KAON would satisfy the needs for all the experiments envisioned here and would provide a suitable hadronic complement to the major nuclear facilities, CEBAF and RHIC.

In the near-term future, there are some opportunities for research with high-energy pion and kaon beams at the Brookhaven AGS. The AGS beam layout is shown in Fig. 21; the proton program is dominated by the rare kaon experiments E787, ($K^+ \to \pi^+\nu\bar{\nu}$), located at LESB-III (C4); E871 ($K_L^0 \to \mu e$), (B5) and E865 ($K^+ \to \pi^+\mu^+e^-$), (A2). In 1996, the E821 (g-2) experiment is expected to be underway.

After the RF cavity upgrades are completed, the AGS should be able to deliver 60×10^{12} protons in a spill, with a 3 second repetition rate. Experimental physics opportunities will be determined by a combination of beam time (anticipated at 26 weeks/year after FY93) and demand; there exists at present opportunities in the LESB-II (C6 and C8) areas and in the D6/8 areas, in the sense that unscheduled beam usage exists for these areas.

The HEPAP recommendations call for the suspension of particle physics support for AGS operations by FY97; the outlook beyond that year is not certain. The availability of the AGS for the kinds of nuclear physics research described here will be strongly dependent on the support and the interest displayed by the U. S. community of intermediate energy users.

Work has been supported under
contract DE-AC02-76CH00016 with
the U.S. Department of Energy.

REFERENCES

[1] "A Proposal to Extend the Intensity Frontier of Nuclear and Particle Physics to 45 GeV," Los Alamos National Laboratory Report LA-UR-84-3982, December 1984; "The Physics and a Plan for a 45 GeV Facility that Extends the High-Intensity Capability in Nuclear and Particle Physics," LA-10720-MS, UC-28 and UC-34, May 1986

[2] KAON Factory Proposal, TRIUMF Report, September 1985

[3] Pilac Users Group Report on the Physics with PILAC, LA-UR-92-150, October 15, 1991

[4] J. R. Sanford and C. L. Wang, Empirical Formulae for Particle Production in P-Be Collision between 10 and 35 BeV/c, Part I, BNL 11299, March 1 1967; Part II, BNL 11479, May 1, 1967.

[5] W. Yamamoto, Study of the the Low-Energy Intense Kaon Beam K2, Thesis, KEK

[6] J. F. Amann et al., "Measurement of Production Cross Sections for Negative Pions, Kaons, and Protons at 10, 18, and 24 GeV," LA-9486-MS, UC-34c, Los Alamos National Laboratory, October 1982

[7] J. A. Holt, M. Takasaki, and K. Nakai, KEK-PS Users Guide Book, KEK National Laboratory for High Energy Physics, 1990

[8] P. H. Pile, private communication, 1992

[9] P. H. Pile et al., Nucl. Instr. and Meth. **A321**, 48 (1992)

[10] P. H. Pile et al., Phys. Rev. Lett. **66**, 2585 (1991)

[11] S. Ajimura et al., Phys. Rev. Lett. **68**, 2137 (1992)

[12] S. Ajimura et al., Phys. Lett. **282B**, 293 (1992)

[13] P. H. Pile, in the LAMPF Workshop on (π, K) Physics, B. F. Gibson, W. R. Gibbs, M. B. Johnson, Eds., AIP Conference Proc. No. 224, Particles and Fields Series 43, p. 77, AIP, New York, (1991)

[14] D. Marlow et al., Phys. Rev. **C30**, 1662 (1984)

[15] D. Marlow et al., Phys. Rev. **C25**, 2619 (1982)

[16] B. M. K. Nefkens, J-C. Peng, and R. E. Chrien, "A New Test of Charge Symmetry in Eta Production on Deuterium," AGS Proposal 890 (1992)

[17] J-C. Peng in Proceedings of πN and NN Physics, p. 315, S. Kruglov, Ed., Gatchina (1989); M. J. Leitch et al., "Performance of a BGO-NaI η Spectrometer," LAMPF Workshop on Photon and Neutral Meson Detection at Intermediate Energies, January 1987 (unpublished)

[18] A. S. Carroll and S. Heppelmann, "EVA, A Solenoidal Detector of Large Angle Exclusive Reactions: Phase I–Determining Color Transparency to 22 GeV/c," AGS Proposal 850 (1988)

[19] A. S. Carroll et al., Phys. Rev. Lett. **61**, 1698 (1988)

[20] Kaon Factory Study- Kaon Factory Science and Experimental Facilities, p. 35, TRIUMF Informal Report, Vancouver, (unpublished)

FIGURES

FIG. 1. The production of positive and negative pions from primary protons at 24.0 GeV/c and at a production angle of 5 deg.

FIG. 2. The production of pions, kaons and antiprotons at the AGS under the same conditions as for Fig. 1

FIG. 3. A comparison of positive pion production at the KEK and the AGS.

FIG. 4. A table of beams available for nuclear physics experiments and the AGS and KEK.

FIG. 5. A spectrum for ^{89}Y showing the positions of the Λ single-particle states.[10]

FIG. 6. The (π^+, K^+) spectrum for carbon[10], indicating the positions of the 1^- states formed by coupling an S-shell Λ to the $(3/2)^-$ neutron hole in ^{12}C.

FIG. 7. The (π^+, K^+) spectrum for a vanadium target. The presence of two sizable neutron valence-hole components, $f_{7/2}$ and $d_{3/2}$, is visible in the spectrum.

FIG. 8. The binding energies and ground state production cross sections as measured

in the second BNL π^+, K^+ experiment[10].

FIG. 9. The running times and experimental parameters for the BNL (π^+, K^+) experiment.

FIG. 10. The polarization detector "ROYAL" developed by Ejiri and his collaborators[11] at KEK.

FIG. 11. A measure of the Λ polarization produced by the quasi-free (π^+, K^+)reaction on ^{12}C.

FIG. 12. The pion-nucleon cross section for the region of the (3,3) resonance and beyond[14]

FIG. 13. Particle time-of-flight spectra produced in the Marlow[15] experiment. The difficulty of distinguishing pions as compared to the relative ease in separating kaons is apparent from the figure.

FIG. 14. The renormalization factors required in the Marlow experiment[14] to produce agreement with the pion-nucleon phase shifts are shown in this figure.

FIG. 15. The apparent dependence of pion time-of-flight on detector size is illustrated

in this figure. The unavoidable presence of a muon halo is responsible for this effect.

FIG. 16. A diagrammatic representation of the eta spectrometer[17].

FIG. 17. The beam layout for AGS Proposal 890, "A test of charge-symmetry-breaking in eta production on deuterium".

FIG. 18. The effect of particle separator tune on pion beam purity. The figure (a) corresponds to a separator *magnetic field of 5 % below and (b) 10 % above optimum tune.*

FIG. 19. The dependence of nuclear transparency on incident proton momentum, as measured at the AGS.[19]

FIG. 20. A set of high energy particle beams as envisaged for the Canadian "KAON" facility.[20]

FIG. 21. A picture of the distribution of AGS beams supplying secondary particles for the experiments of the next few years.

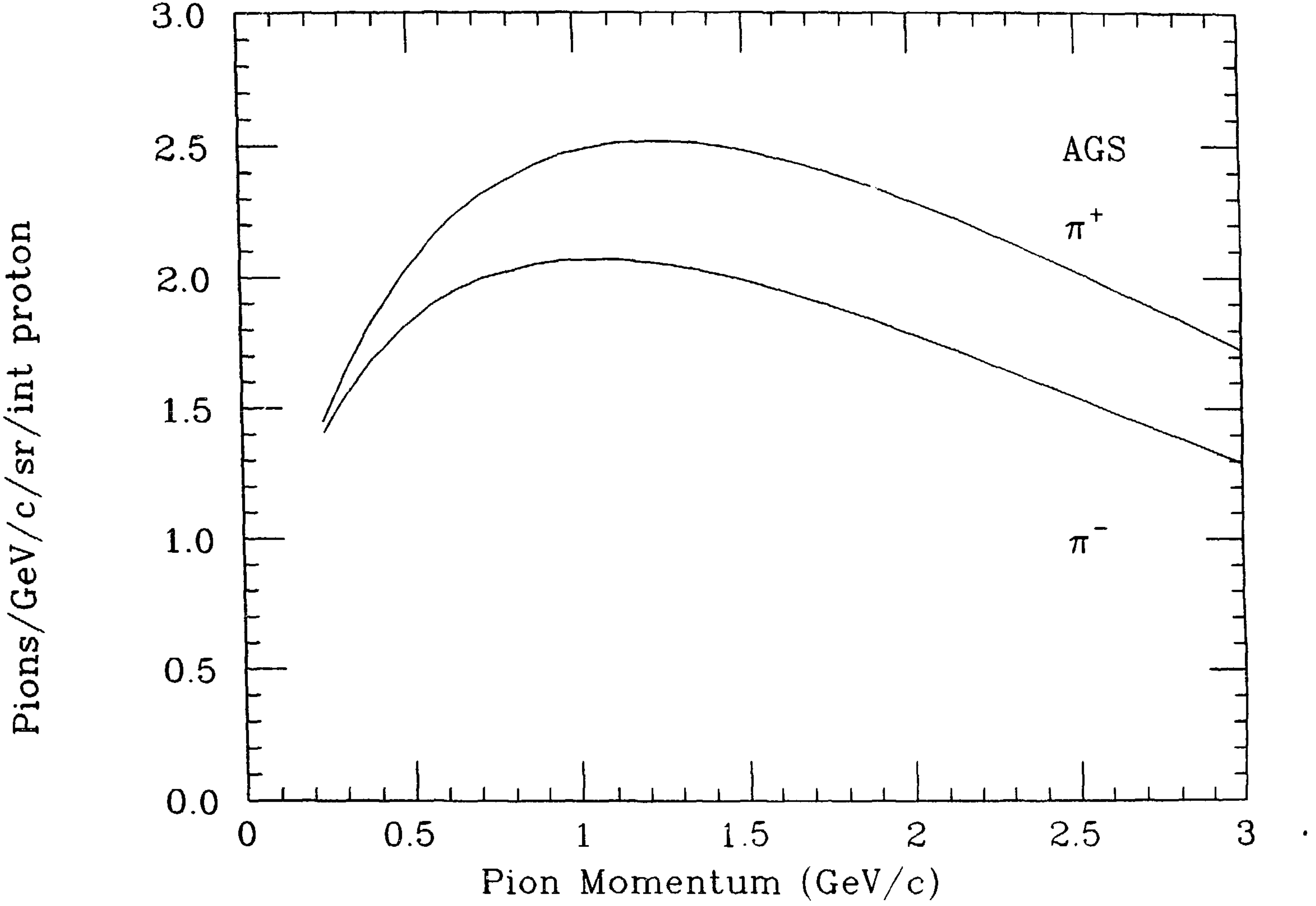
3.0
2.5
2.0
1.5
1.0
0.5
0.0
0
0.5
1
1.5
2
2.5
3
Pions/GeV/c/sr/int proton
Pion Momentum (GeV/c)
AGS
π+
π−

fig 1

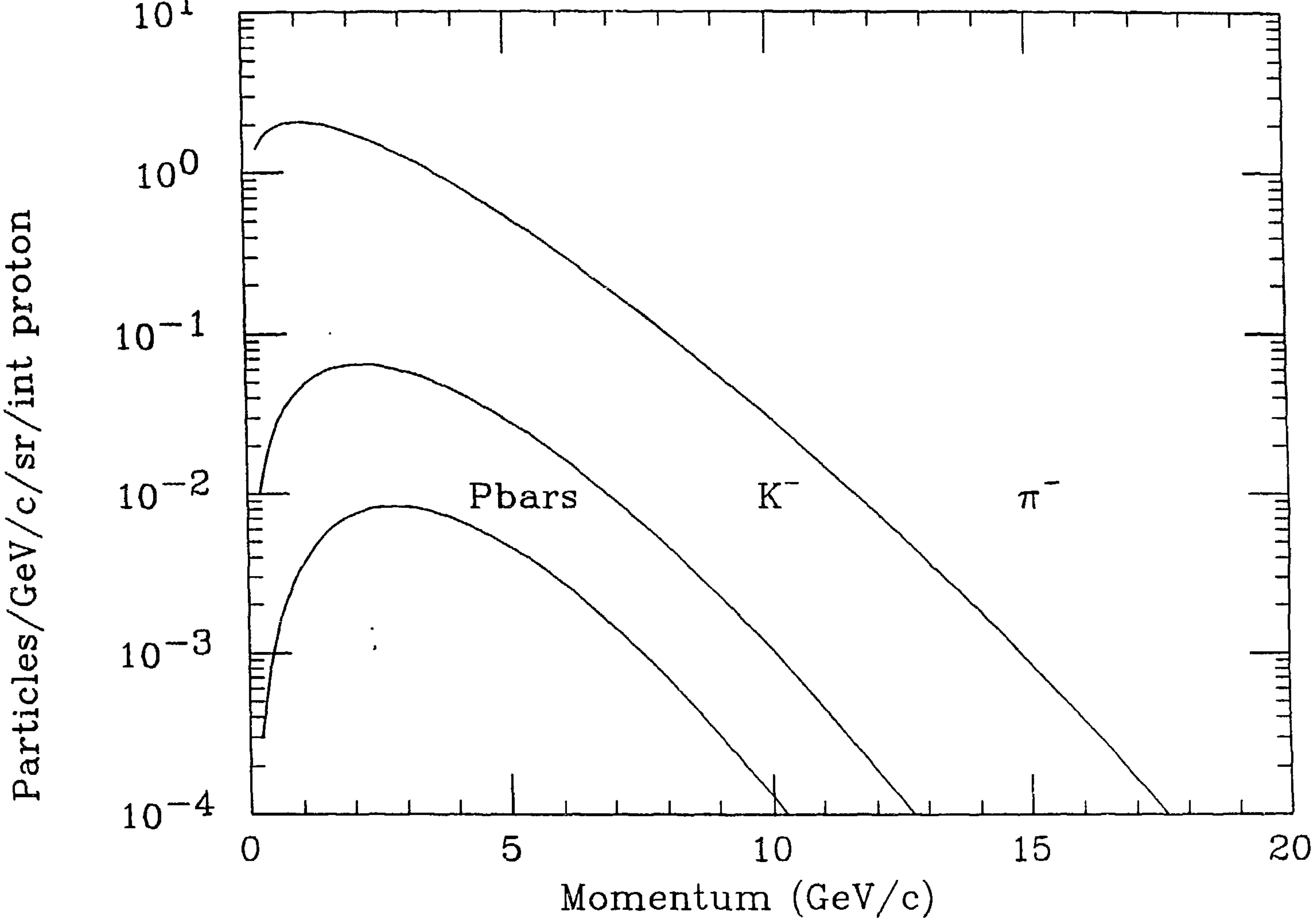

10^1
10^0
10^{-1}
10^{-2}
10^{-3}
10^{-4}
Particles/GeV/c/sr/int proton
Pbars
K^-
π^-
0
5
10
15
20
Momentum (GeV/c)

Fig 2

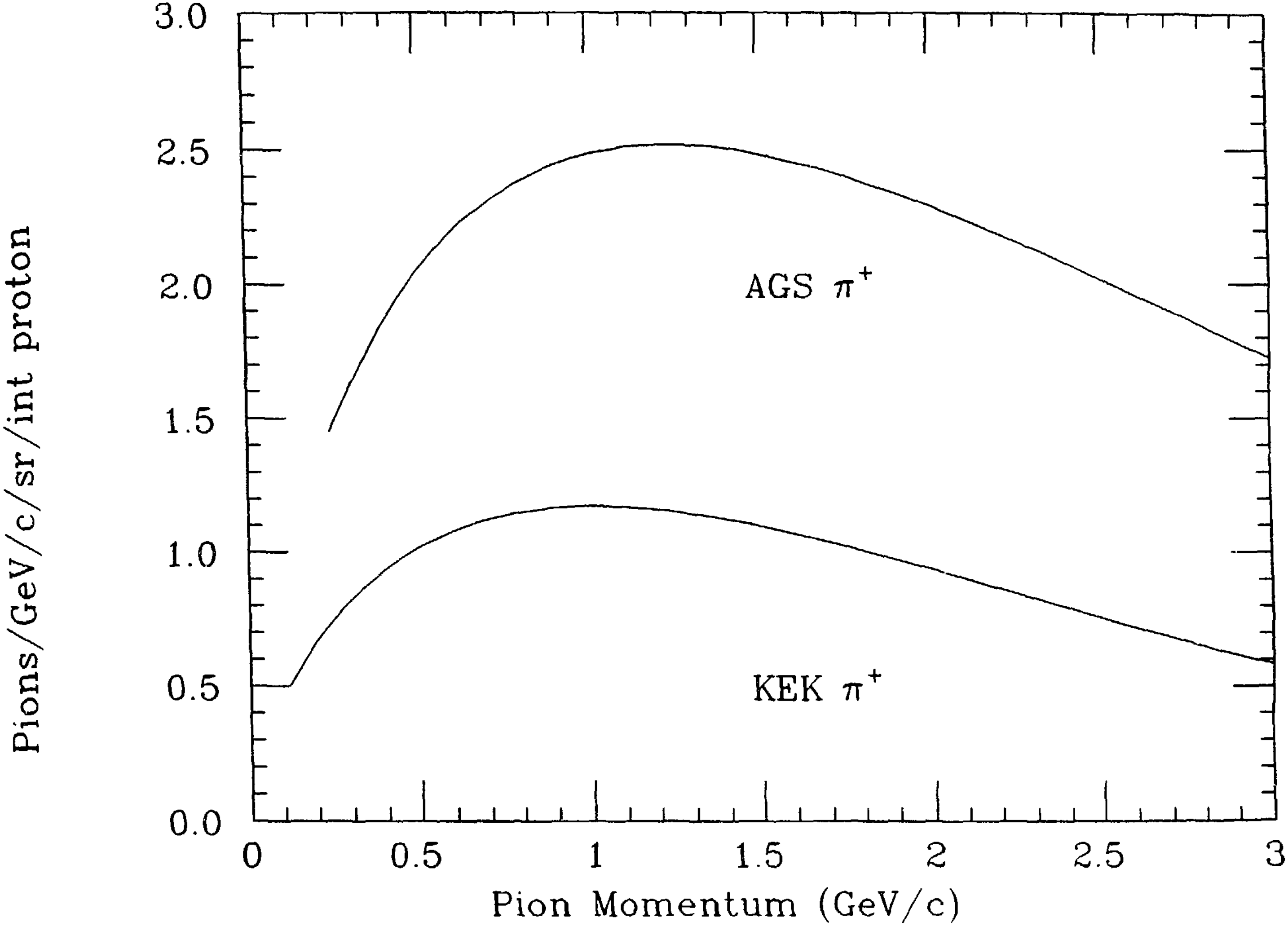
3.0
2.5
2.0
1.5
1.0
0.5
0.0
Pions/GeV/c/sr/int proton
0
0.5
1
1.5
2
2.5
3
Pion Momentum (GeV/c)
AGS π^+
KEK π^+

Fig. 3

Presently Available Beam Lines

				Intensity in 10^6 particles per 10^{13} protons		
		p_{max}	$\delta p/p_o$	π^+	K^+	$\bar{p}$
1)	AGS-LESBIII	.85	4	6000	4.6	0.21
2)	AGS-LESBII	.75	5	6000	3.0	0.14
3)	AGS-D6	1.8	6	600	6.7	1.3
*4)	AGS-A1	28	3	30 @ 18 GeV/c		
*5)	AGS-A2	6.5	5	740 @ 6 GeV/c		
*6)	AGS-A3	28	4	100 @ 14 GeV/c		
† *7)	AGS C-1	20	5	350 @ 13 GeV/c		
8)	KEK-K2	2	6	220	5	0.15
9)	KEK-K3	1	5	500	0.4	0.0035 @ 0.55
10)	KEK-K5	0.6	6	600	1.2	.08
11)	KEK-K6	2.0	5.6	380	7	0.26
*12)	KEK π2	4.0	2	2 @ 3 GeV/c		
*13)	KEK T1	2.0	10	0.5 @ 1 GeV/c		
*14)	KEK T3	6	10	1.0 @ 5 GeV/c		

*unseparated beams

†proton intensity 10^9

Fig 4

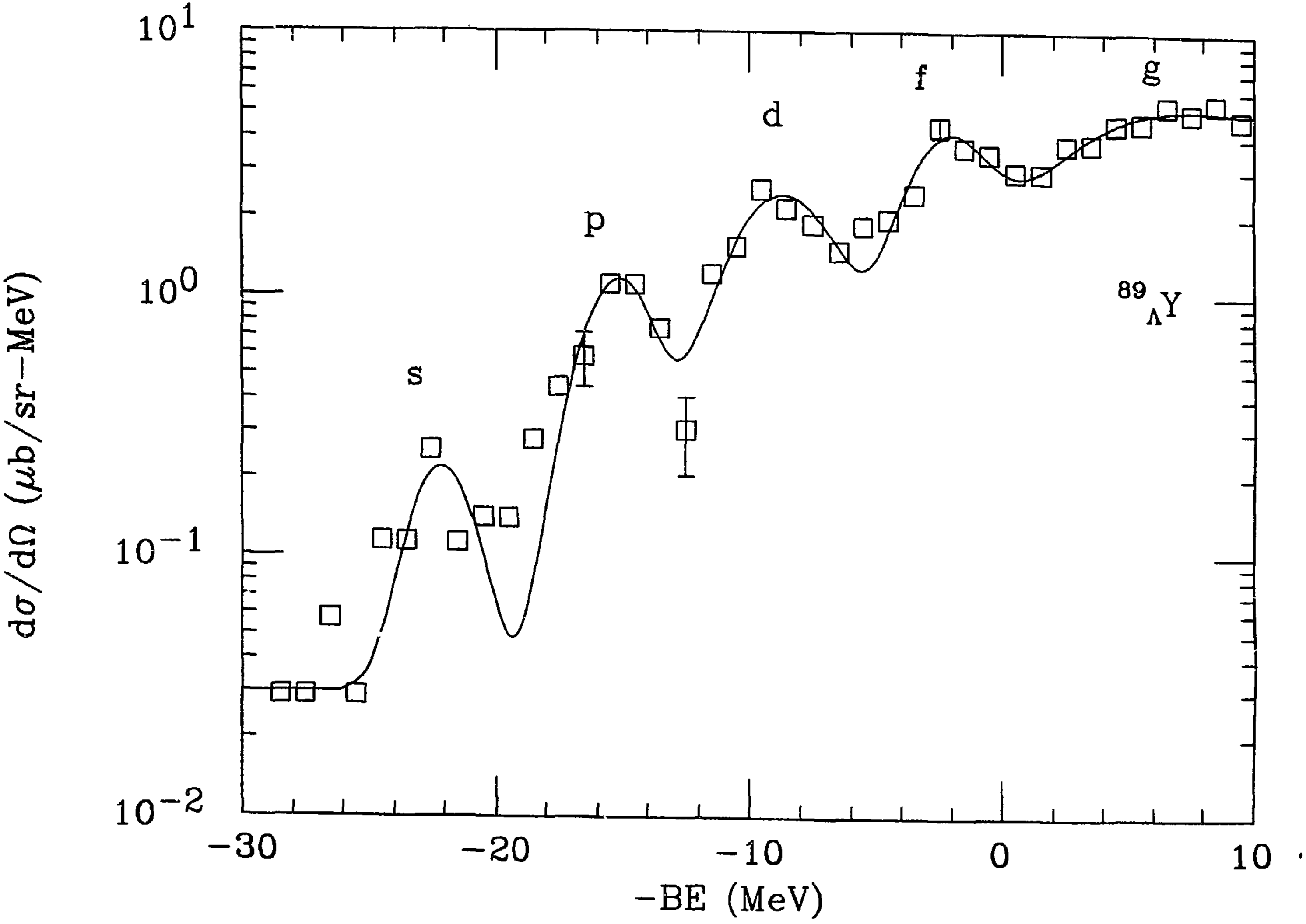
10^1
10^0
10^{-1}
10^{-2}
$d\sigma/d\Omega$ (μb/sr−MeV)
−30
−20
−10
0
10
−BE (MeV)
s
p
d
f
g
$^{89}_{\Lambda}Y$

fig 5

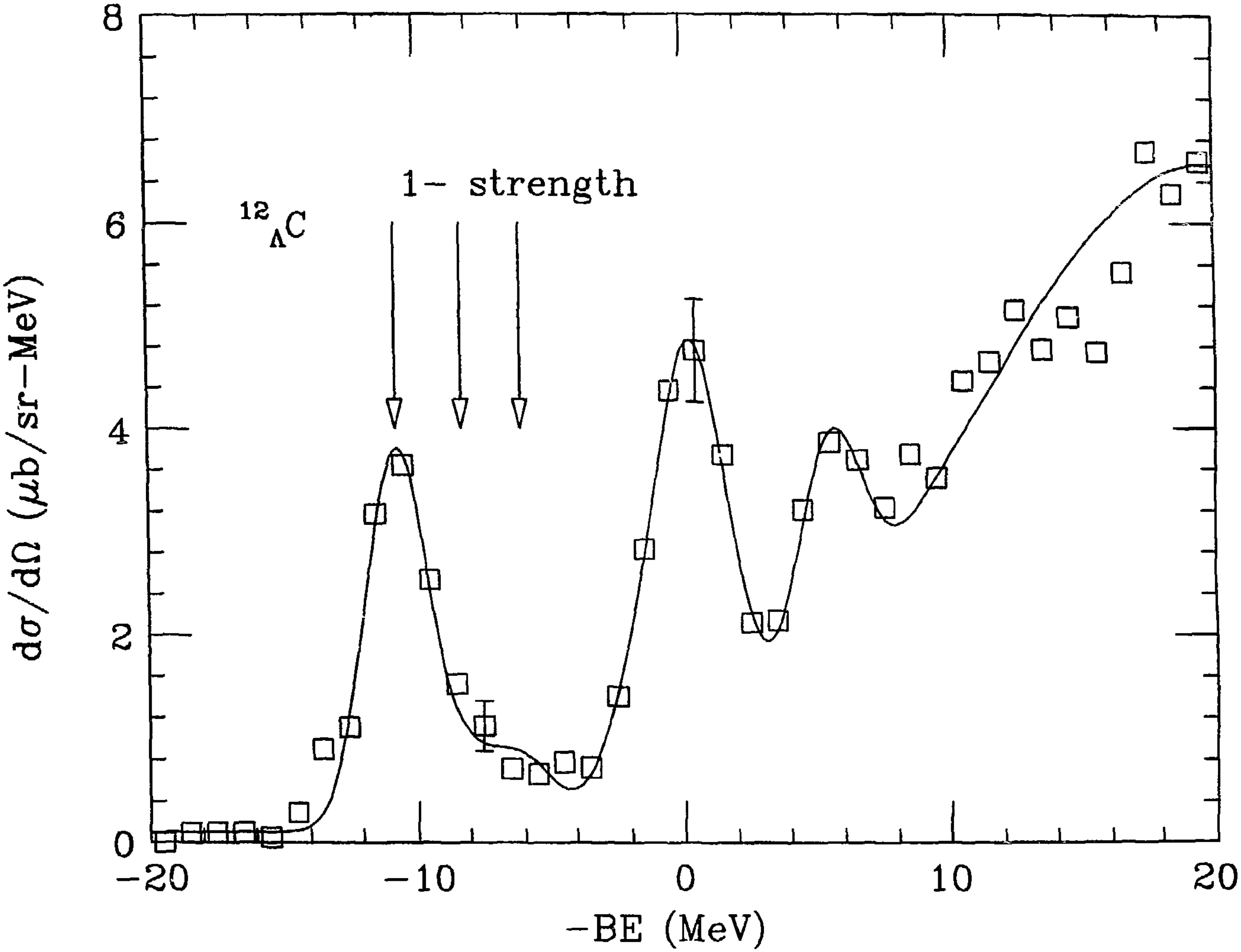

fig 6

fig 7

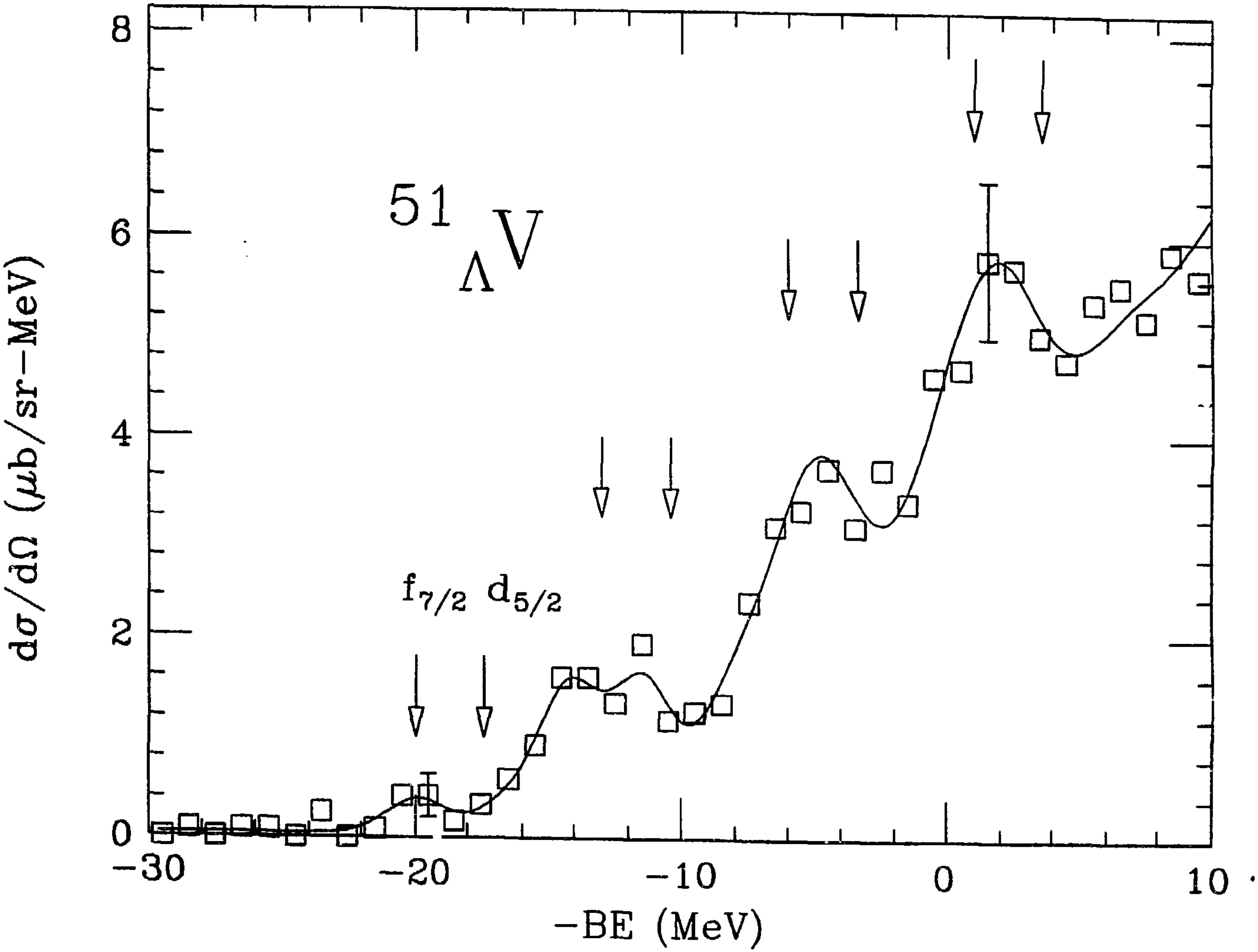

Nucleus	BE (MeV)	σ (μb/sr)
${}^{9}_{\Lambda}\mathrm{Be}$	6.49 ± 0.68	0.87 ± 0.34
${}^{12}_{\Lambda}\mathrm{C}$	10.75 ± 0.10	10.36 ± 0.61
${}^{16}_{\Lambda}\mathrm{O}$	12.50 ± 0.35	1.68 ± 0.36
${}^{28}_{\Lambda}\mathrm{Si}$	16.00 ± 0.29	2.06 ± 0.34
${}^{40}_{\Lambda}\mathrm{Ca}$	18.70 ± 1.1	0.48 ± 0.28
${}^{51}_{\Lambda}\mathrm{V}$	19.9 ± 1.0	1.00 ± 0.56
${}^{89}_{\Lambda}\mathrm{Y}$	22.1 ± 1.6	0.54 ± 0.38

Fig 8

A summary of the experimental running conditions and targets used. The incident beam momentum was $p_\pi = 1048$ MeV/c. The data were taken at $\theta_{\mathrm{lab}} = 10°$ with the spectrometer set for $p_K = 700$ MeV/c.

Target	Thickness (g/cm^2)	Run time (h)	π^+ intensity on target (per spill)[a]
^{9}Be	2.35	27	2×10^{6}
^{12}C	2.0	13.5	2×10^{6}
^{16}O[b]	3.0	43.4	2×10^{6}
^{28}Si[c]	4.03	73.3	2×10^{6}
^{40}Ca[c]	4.13	109.5	(2 and 10)$\times10^{6}$
^{51}V[d]	3.48	23	10×10^{6}
^{89}Y	3.95	88	10×10^{6}

[a] The AGS beam spill length for this experiment was about 1.2 s with a 2.9-s repetition rate.

[b] In water.

[c] Natural target.

[d] Run in tandem with a ^{13}C target.

fig 9

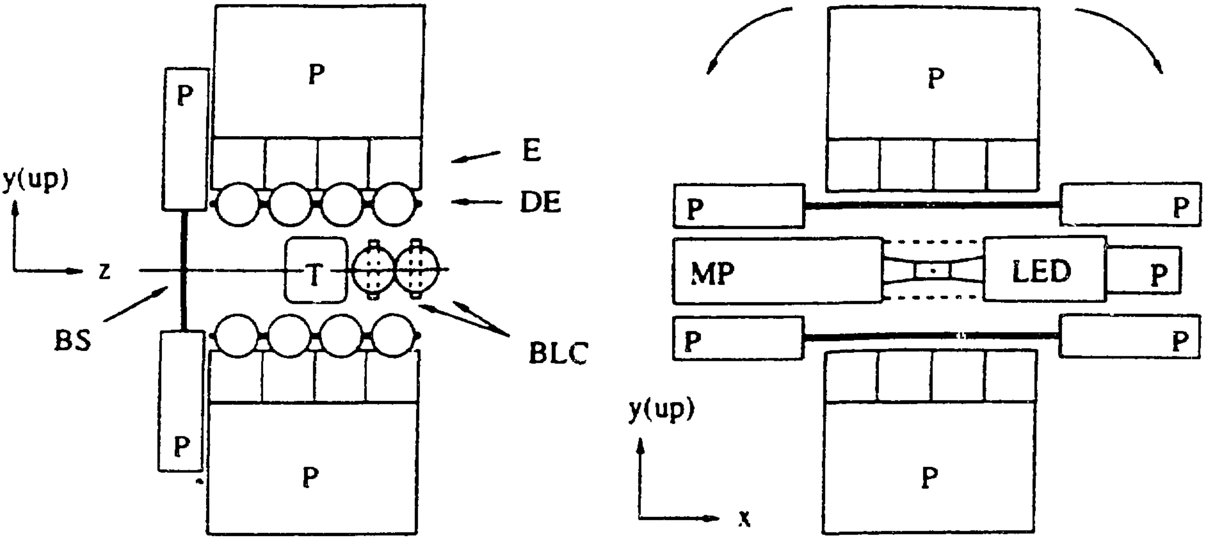

side view

front view

fig 10

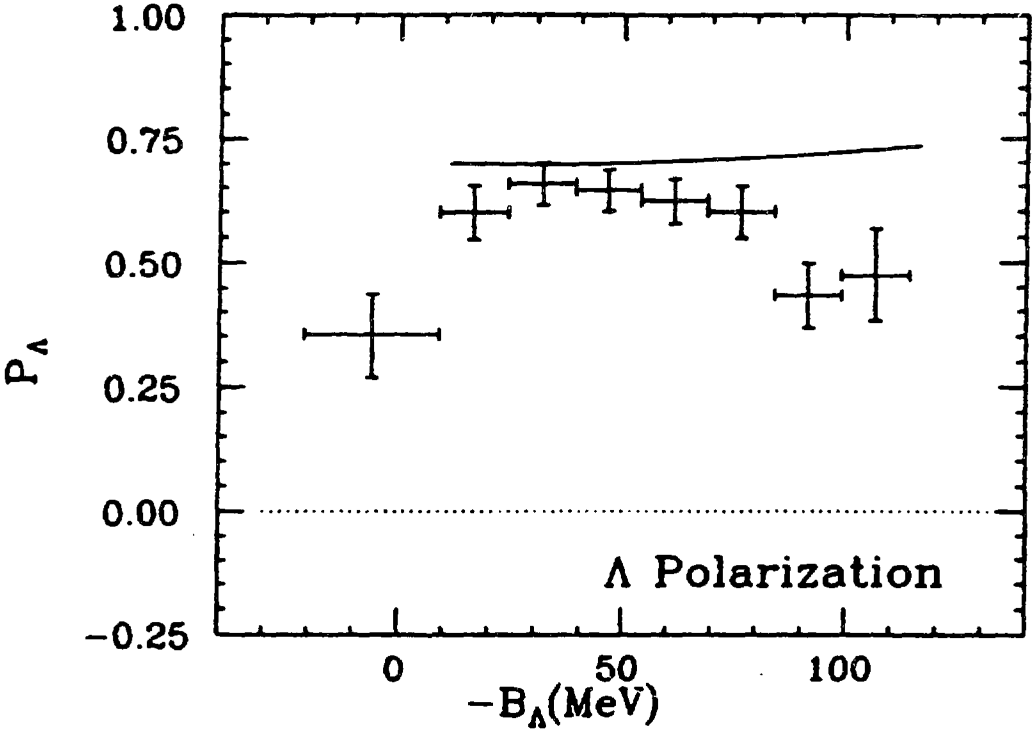
1.00
0.75
0.50
0.25
0.00
−0.25
P_Λ
Λ Polarization
0
50
100
$-B_\Lambda$(MeV)

fig 11

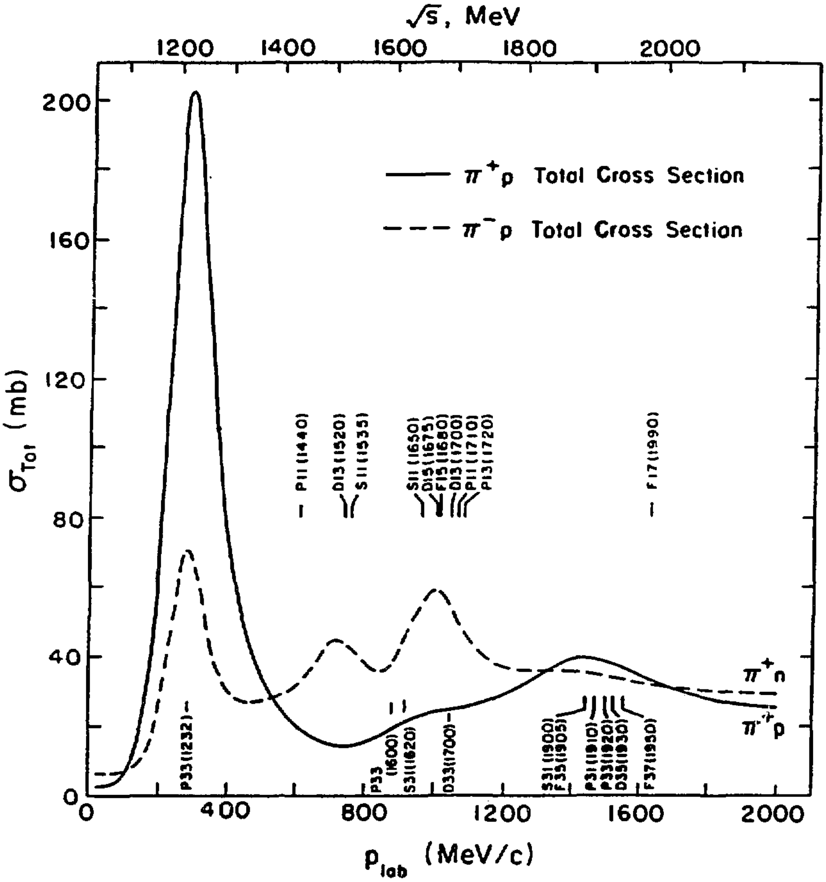
√s, MeV
1200
1400
1600
1800
2000
200
160
120
80
40
0
σ_Tot (mb)
π⁺p Total Cross Section
π⁻p Total Cross Section
P11(1440)
D13(1520)
S11(1535)
S11(1650)
D15(1675)
F15(1680)
D13(1700)
P11(1710)
P13(1720)
F17(1990)
P33(1232)
P33
(1600)
S31(1620)
D33(1700)
S31(1900)
F35(1905)
P31(1910)
P33(1920)
D35(1930)
F37(1950)
π⁺n
π⁺p
0
400
800
1200
1600
2000
p_lab (MeV/c)

Fig 12

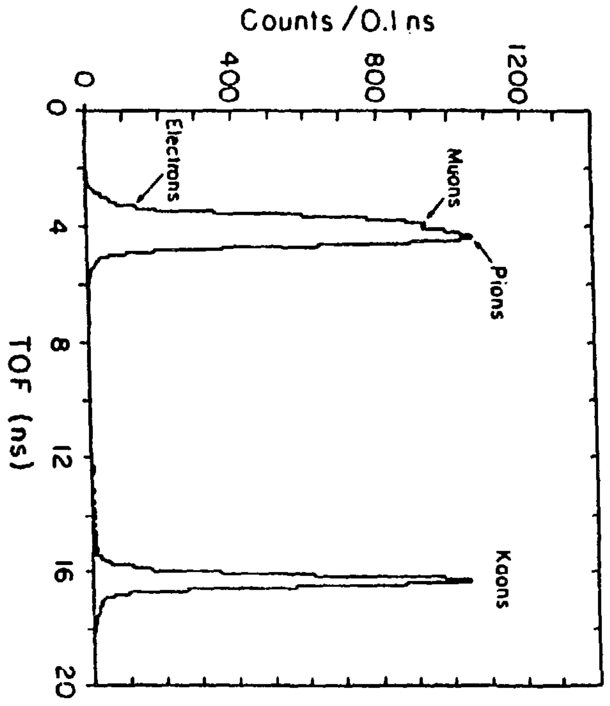
Counts /0.1 ns
0
400
800
1200
0
4
8
12
16
20
TOF (ns)
Electrons
Muons
Pions
Kaons

fig 13

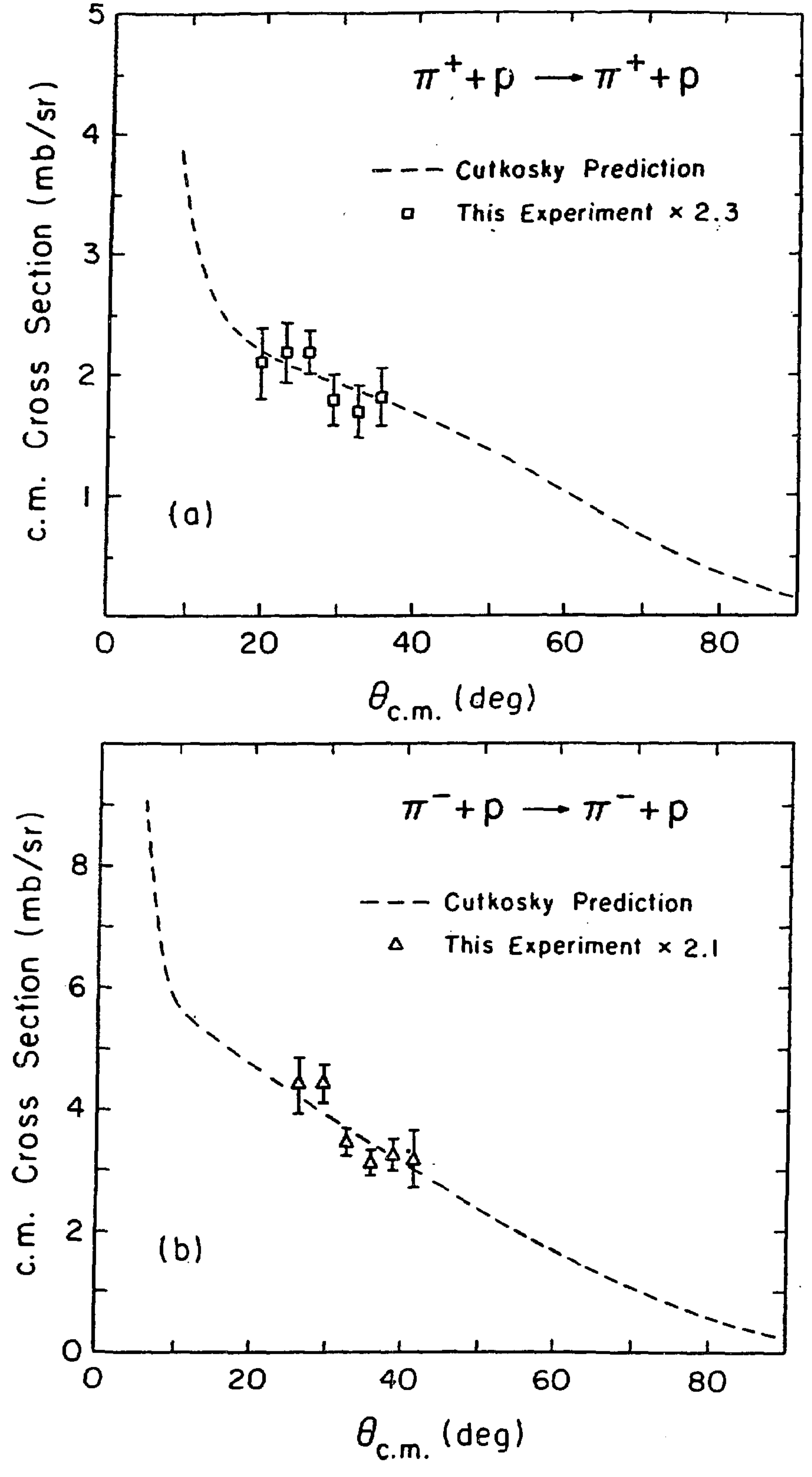

$\pi^+ + p \rightarrow \pi^+ + p$
Cutkosky Prediction
This Experiment × 2.3
(a)
c.m. Cross Section (mb/sr)
0
1
2
3
4
5
20
40
60
80
$\theta_{c.m.}$ (deg)
$\pi^- + p \rightarrow \pi^- + p$
Cutkosky Prediction
This Experiment × 2.1
(b)
c.m. Cross Section (mb/sr)
0
2
4
6
8
20
40
60
80
$\theta_{c.m.}$ (deg)

fig 4

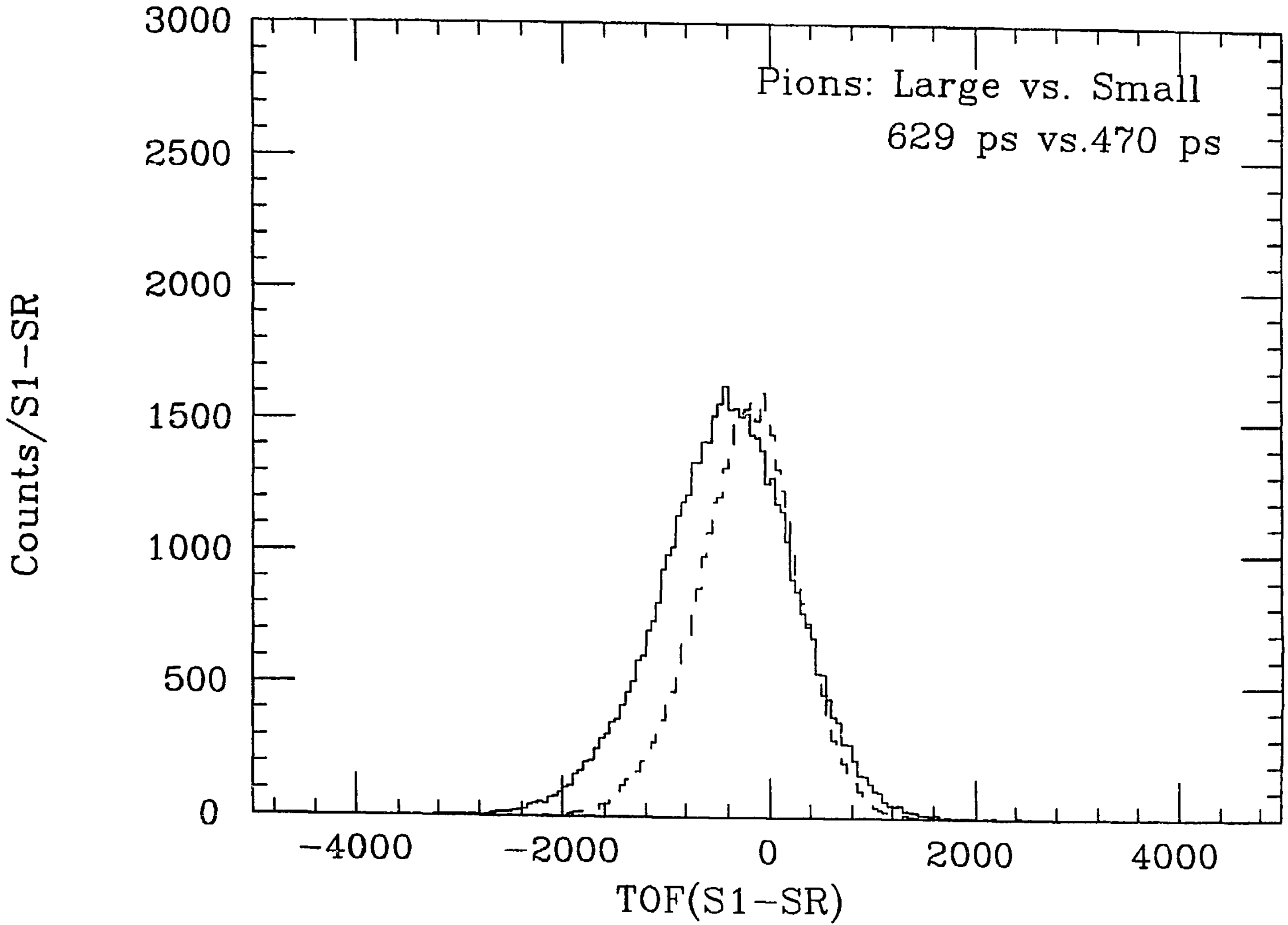
Pions: Large vs. Small
629 ps vs.470 ps
Counts/S1−SR
3000
2500
2000
1500
1000
500
0
−4000
−2000
0
2000
4000
TOF(S1−SR)

fig 15

ETA SPECTROMETER
(EXPLODED VIEW)

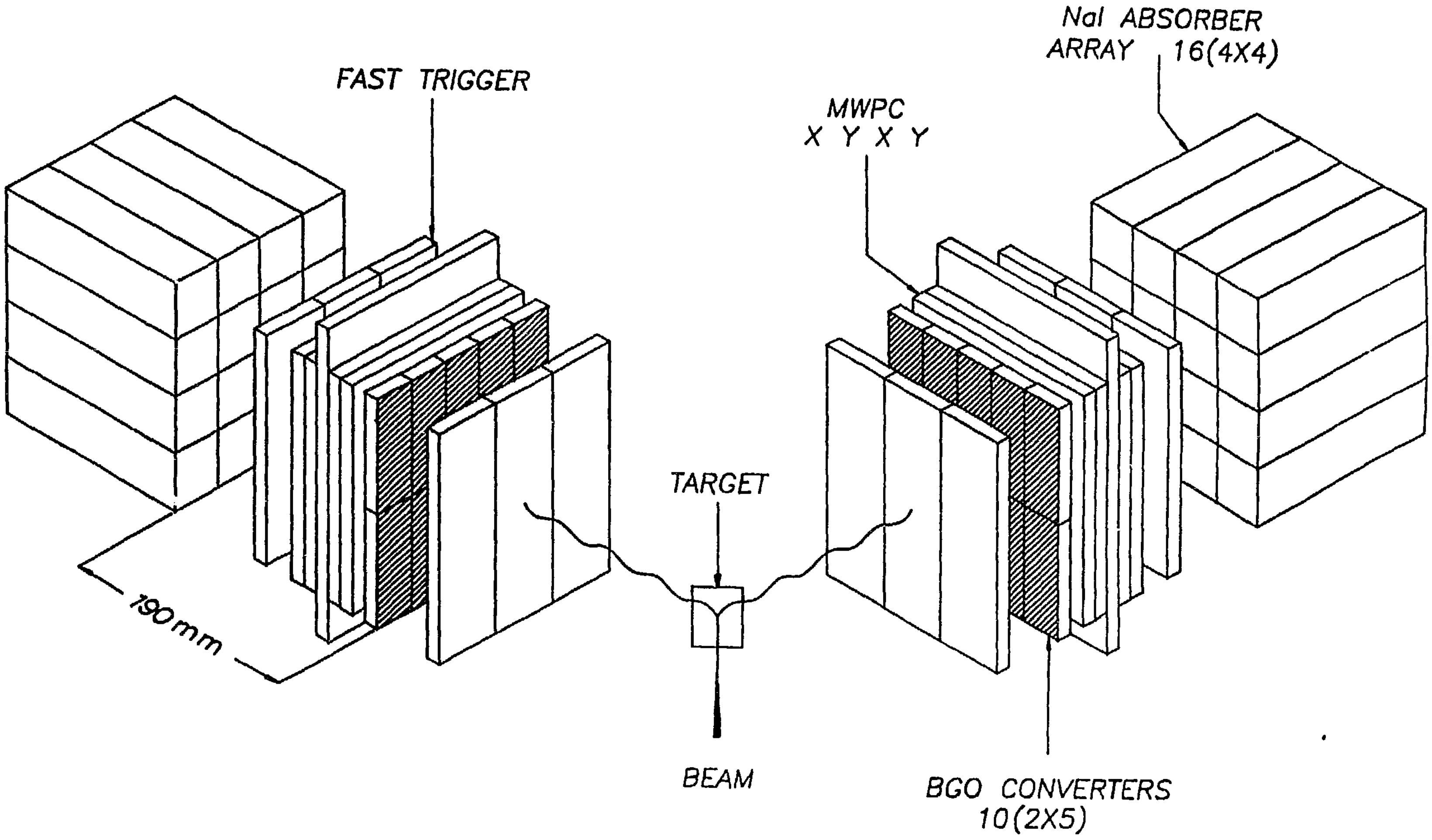

Fig 16

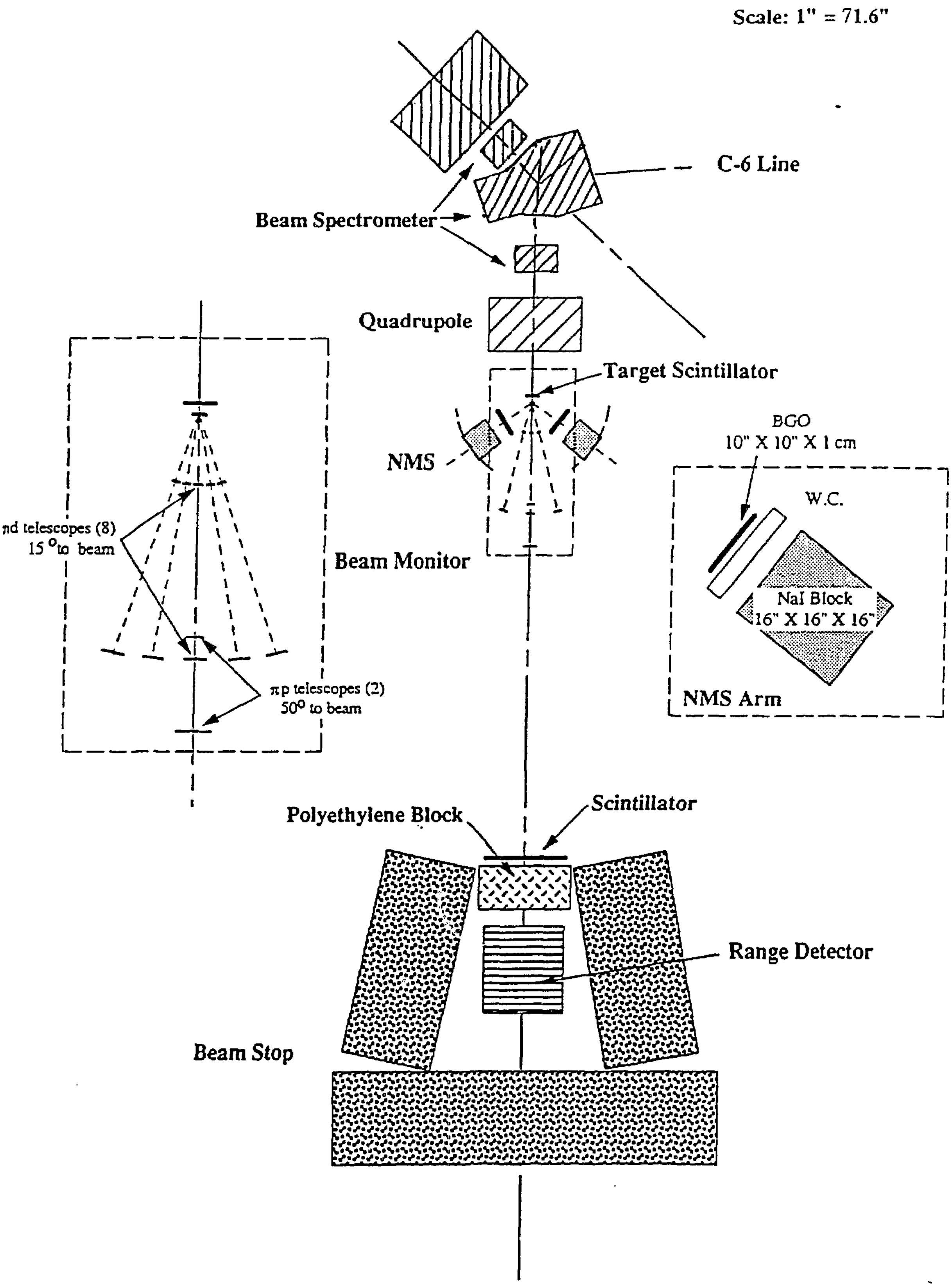
Scale: 1" = 71.6"
C-6 Line
Beam Spectrometer
Quadrupole
Target Scintillator
NMS
BGO
10" X 10" X 1 cm
W.C.
NaI Block
16" X 16" X 16"
NMS Arm
πd telescopes (8)
15 ° to beam
Beam Monitor
πp telescopes (2)
50° to beam
Polyethylene Block
Scintillator
Range Detector
Beam Stop

fig 17

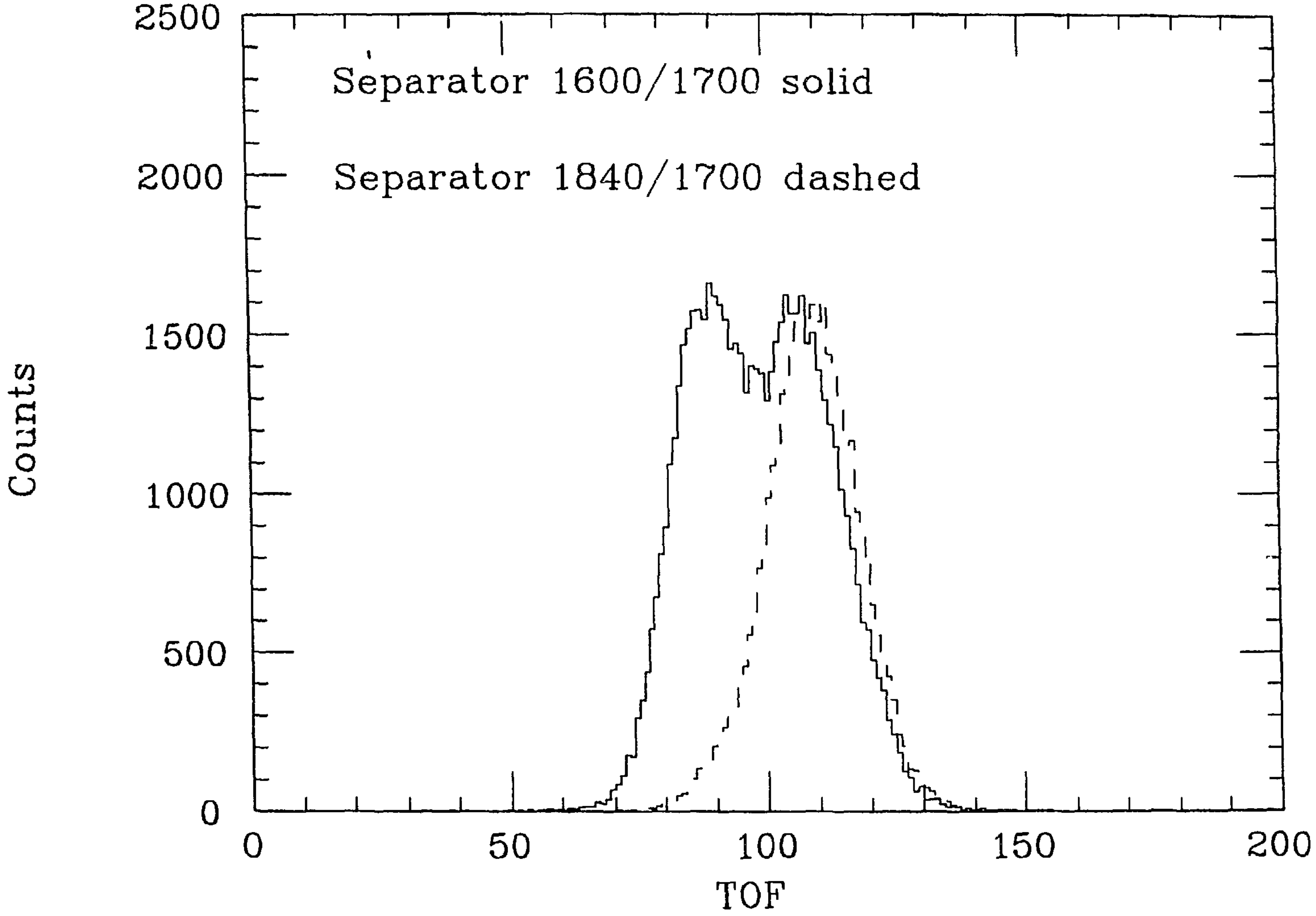
Separator 1600/1700 solid
Separator 1840/1700 dashed
Counts
2500
2000
1500
1000
500
0
0
50
100
150
200
TOF

fig 16

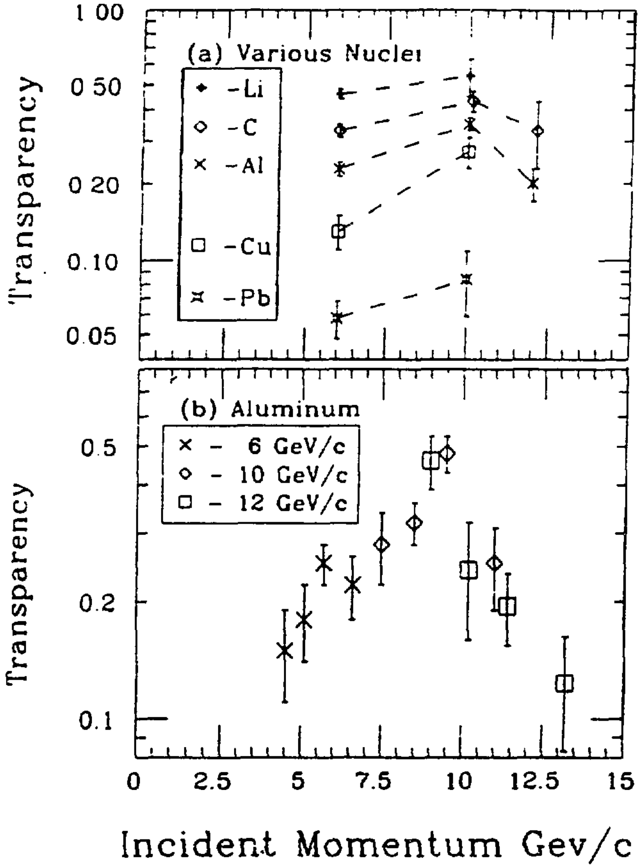
(a) Various Nuclei
-Li
-C
-Al
-Cu
-Pb
Transparency
1.00
0.50
0.20
0.10
0.05
(b) Aluminum
× - 6 GeV/c
◇ - 10 GeV/c
□ - 12 GeV/c
Transparency
0.5
0.2
0.1
0
2.5
5
7.5
10
12.5
15
Incident Momentum Gev/c

fig 19

Properties of Separated Beams at KAON

Channel	Momentum GeV/c	Solid Angle msr	Momentum Acceptance $\Delta p/p$ in %	Length m	Type of Separation
K20	20 -6	0.1	1	160	RF, 3 cavities, 2.8 GHz
K6	6 -2.5	0.08-0.30	3	110	RF, 3 cavities, 1.3 GHz
K2.5	2.5 -1.25	0.5 -2.0	4	54	DC, 2 stages
K1.5	1.5 -0.75	2.0	4	30	DC, 2 stages
KO.80	0.80-0.55	6.0	5	18	DC, 2 stages
KO.55	0.55-0.40	8.0	6	14	DC, 1 stage, extra optics

Anticipated Beam Intensities[a]

Channel	P GeV/c	K^- 10^6/s	K^+ 10^6/s	π^- 10^9/s	π^+ 10^9/s	$\bar{p}$ 10^6/s
K20	21	0.75	29	0.16	0.95	0.05
	18	2.4	43	0.35	1.05	0.35
	15	5.9	62	0.60	1.50	1.7
	12	9.2	52	0.90	1.90	5.0
	9	7.9	23	0.70	1.30	10.5
	6	2.3	4.2	0.78	1.20	11.5
K6	6	15	34	1.9	3.6	23
	3	2.5	4.5	3.2	5.0	43
K2.5	2.5	66	119	16	24	110
	2.0	39	76	21	30	91
	1.5	14	27	25	36	52
	1.25	5.4	9.7	27	37	26
K1.5	1.5	193	366	49	69	81
	1.2	52	93	36	49	25
	1.0	18	31	27	36	8.3
	0.8	3.7	6.3	18	23	1.9
K0.8	0.8	99	203	87	113	7.1
	0.65	32	59	63	80	2.6
	0.55	10	19	44	55	1.0
K0.55	0.55	41	80	80	101	1.5
	0.50	21	44	67	82	0.93
	0.45	9.2	21	50	61	0.53
	0.40	3.8	9.4	33	44	0.30

---

[a] Intensities are for a 100 μA 30 GeV beam on a 6 cm Pt target.

fig 2c

AGS Experimental Area
High Energy Physics FY1993
4 June 92

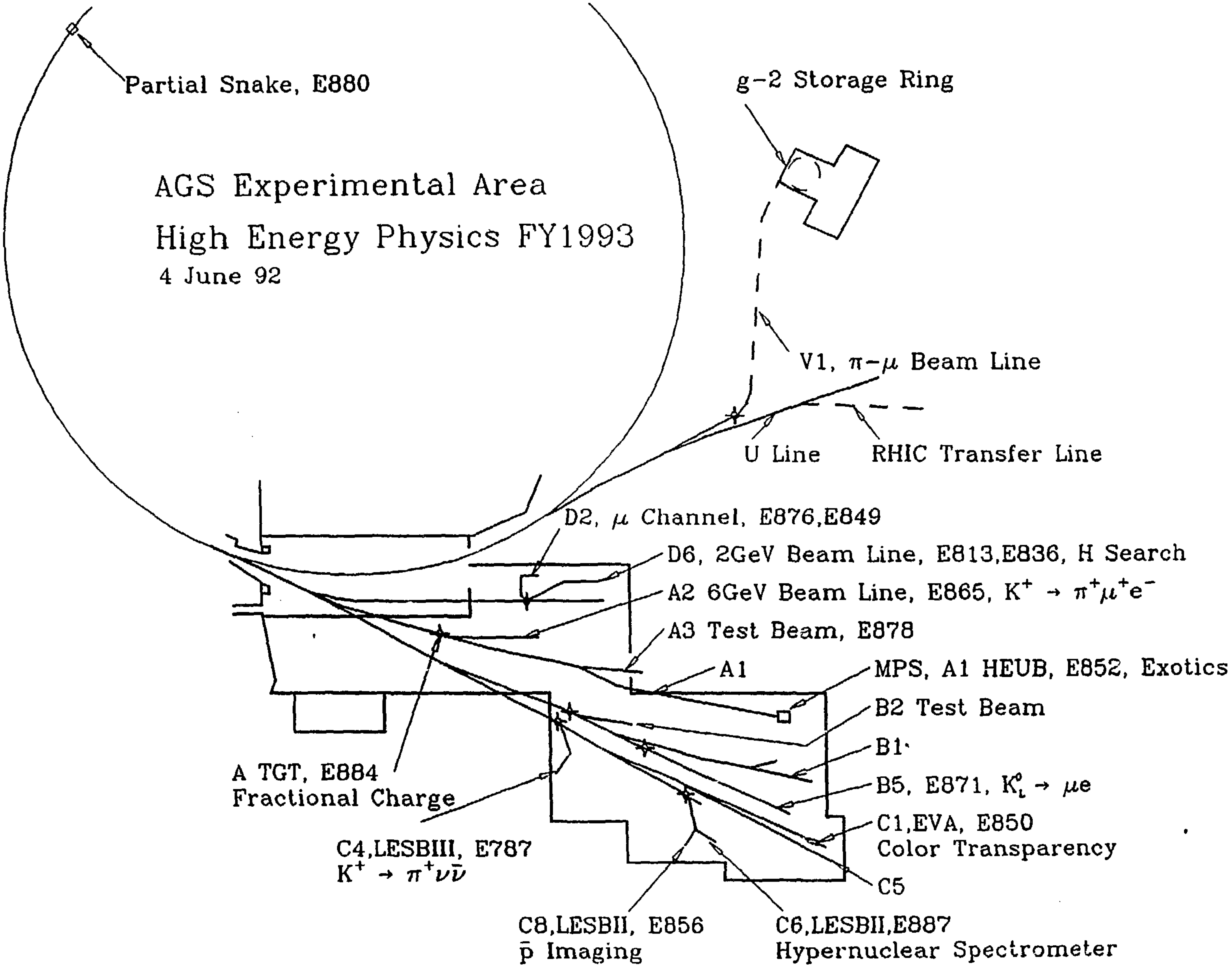

Fig 21

TECHNICAL INFORMATION DIVISION

PUBLICATIONS

Contact Person: J. Mooney

Author: R. E. Chrien

We are unable to process your paper because the following paperwork/information is missing:

______ TID report processing form (BNL F 2843B)

______ Author's statement (BNL F 167D)

______ DOE form F - 1332.15

______ DOE form F - 1340.3

______ NRC form - 426A

______ NRC form - 335

___✓___ **Credit Line** - DEAC02-76CH00016

______ Copyright statement

______ DOE UC category code

Please return with the completed paperwork/information as soon as possible.

Date returned from Dept.________